ELSEVIER

Chemical Physics 236 (1998) 181–188

Chemical Physics

On the $O_2(v') + O_2(v'')$ atmospheric reaction. II. The role of rotational excitation

W. Wang, A.J. C. Varandas

Departamento de Química, Universidade Coimbra, P-3049 Coimbra Codex, Portugal

Received 13 October 1997; in final form 12 March 1998

Abstract

The effect of rotational excitation on the rate constant for the title reaction is investigated by using the quasiclassical trajectory method and the realistic double many-body expansion (DMBE) potential energy surface for ground-state triplet O_4. The results are compared with previously reported calculations in which such effects have been neglected.

1. Introduction

Ozone plays a key role in stratospheric and mesospheric chemistry, and hence the understanding of the processes that determine its concentration is of considerable interest. In particular, the so-called "ozone deficit" problem has been the object of much debate (Refs. [1–3], and references therein). Indeed, numerous studies have failed to find the expected agreement between odd oxygen (i.e., O and O_3) production and destruction. To account for a surplus in odd oxygen, Wodtke and coworkers [2,4,5] suggested that the rapid bimolecular reaction between vibrational excited $O_2(v \geq 26)$ and ground state O_2 leads to ozone formation through the following mechanism

$$O_3 + h\nu(\lambda < 243\,\text{nm}) \rightarrow O_2\left(X\,^3\Sigma_g^-, v\right) + O(^3P), \tag{1}$$

$$O_2\left(X\,^3\Sigma_g^-, v' \geq 26\right) + O_2\left(X\,^3\Sigma_g^-, v'' = 0\right) \rightarrow O_3 + O(^3P), \tag{2}$$

$$O(^3P) + O_2 + M \rightarrow O_3 + M. \tag{3}$$

This mechanism has been used to explain some experimental results on the vibrational relaxation study of $O_2(v)$ molecules [4–8], but a direct observation of the ozone formation has not been provided. Theoretically, Balakrishnan and Billing [9] have calculated the cross sections and rate constants for the title reaction for the vibrational combinations (26,0), (27,0) and (30,0) using the DMBE potential energy surface [10] for ground triplet $O_4(^3A)$ and a semiclassical wavepacket [11] approach, and demonstrated that no reaction occurs in the energy range and vibrational combinations used in their work. Most recently, from model calculations of vibrational self-relaxation rates of high vibrationally excited oxygen molecules carried out on the DMBE potential energy surface, Campos-Martinez et al. [12] have suggested that the observed jump in $O_2(v)$ depletion is due to pure inelastic collisions, rather than to ozone formation. Moreover, they have noted that the geometry of the transition state on the DMBE potential energy surface agrees well with the results from recent *ab initio* calculations [13]. Thus, except for some disagreement with experiment in the descrip-

0301-0104/98/$ - see front matter
PII: S0301-0104(98)00164-5

tion of the rotational distribution and role of the spectator bond (the one which is not broken or formed during the course of the reaction) for the inverse $O + O_3$ reaction [14], the O_4 DMBE potential energy surface stems as a fairly reliable model on which to carry out dynamics studies of the important title reaction.

In a previous paper [15] (hereafter referred to as paper I), we have suggested a related mechanism for O_3 production in which reaction (2) is replaced by

$$O_2\left(X^3\Sigma_g^-,v'\right) + O_2\left(X^3\Sigma_g^-,v''\right) \rightarrow O_2 + O(^3P) + O(^3P), \quad (4)$$

while maintaining reactions (1) and (3). Note that in paper I we have also considered the process

$$O_2\left(X^3\Sigma_g^-,v'\right) + O_2\left(X^3\Sigma_g^-,v''\right) \rightarrow O_3^\star + O(^3P), \quad (5)$$

where the star indicates that the formed ozone has an internal energy above the dissociation limit which may dissociate to give an oxygen atom and an oxygen molecule or stabilize in the presence of some inert species to give a stable ozone molecule (as predicted from our calculations in Ref. [15], direct formation of stable ozone is unlikely to occur to a significant extent). Thus, in the generalized mechanism of paper I, reactions (4) and (5) must be considered as alternatives to reaction (2). Our mechanism differs therefore from that suggested by Wodtke and coworkers [2] in that it accounts for all collision processes in which one or both O_2 molecules are vibrationally excited. As stated in Ref. [15], for being of relevance in the stratospheric ozone chemistry, the mechanism must rely on the assumption of non-local thermodynamical equilibrium (non-LTE) to increase the probability of bringing together two vibrationally hot oxygen molecules to react. Indeed, the non-LTE hypothesis has been recognized [16] as taking place in such regions of the atmosphere. Moreover, there are other sources of vibrationally excited oxygen molecules in the stratosphere besides Eq. (1), e.g., $O + HO_2 \rightarrow O_2(v) + OH$ where the product oxygen molecules have been found [17] to be vibrationally excited up to $v = 13$. However, in paper I we have calculated the cross sections and thermal rate coefficients for reactions (4) and (5) by considering both colliding O_2 molecules on their ground rotational levels, $j' = j'' = 1$. Because such an assumption has been questioned in that paper, a study of the effect of rotational excitation on the kinetics of the title reaction has been undertaken in our group. A major aim of the present work is therefore to report the results of the investigation that we have carried out towards such a goal. Of course, besides its relevance in atmospheric chemistry, the title reaction can be interesting *per se* as a prototype of a bimolecular collision process involving vibrationally hot oxygen molecules.

The plan of the paper is as follows. Section 2 summarizes the computational approach and the basic formulas employed. The results and discussion are presented in Section 3. Section 4 gathers some conclusions.

2. Method

As in paper I, all calculations have employed the quasiclassical trajectory (QCT) method using an extensively adapted version of the MERCURY [18] computer program. Similarly, we use the six-dimensional single-valued DMBE [19,20] potential energy surface [10] for ground-state triplet O_4, which has also been used in studies [10,14,15,21,22] of the reaction

$$O(^3P) + O_3(^1A_1) \rightarrow 2O_2\left(X^3\Sigma_g^-\right). \quad (6)$$

All parameters required for the dynamics calculations have been optimized according to common practice.

The rotational specific (j',j'') rate constant for a specified vibrational combination (v',v'') can be calculated using the expression

$$k^x_{v'v''j'j''}(T) = g_e\left(\frac{8kT}{\pi\mu_{O_2-O_2}}\right)^{1/2}\left(\frac{1}{kT}\right)^2 \times \int_0^\infty \int_0^{b_{max}} P^x_{v'v''j'j''}(E_{tr},b)\exp(-E_{tr}/kT) \times 2\pi b\,db\,E_{tr}\,dE_{tr}, \quad (7)$$

where, following paper I, $x = \star$, 'dir', 'diss', 'exc'

stands for excited ozone formation, stable ozone formation, direct dissociation into $O_2 + O + O$, and oxygen-atom exchange. Moreover, $g_e = 1/3$ is the electronic degeneracy factor, k is the Boltzmann constant, and $\mu_{O_2-O_2}$ is the reduced mass of the colliding pair. To obtain the rate constants, the integrals in Eq. (7) have been evaluated using a direct QCT approach, according to which the initial translational energy (E_{tr}) of each trajectory is randomly generated such as to mimic the Maxwell-Boltzmann distribution at a given temperature. Thus, we define the reactive cross section, $\sigma^x_{v'v''j'j''}(T)$, for a given temperature by

$$\sigma^x_{v'v''j'j''}(T) = \pi b^2_{max}(T) P^x_{v'v''j'j''}(T), \tag{8}$$

where the reactive probability (i.e., the ratio of the number of reactive and total trajectories) for the initial combination (v',v'',j',j'') is defined as $P^x_{v'v''j'j''}(T) = N^x_{v'v''j'j''}(T)/N_{tot}$, and the statistical 68% confidence interval is given by

$$\Delta\sigma^x_{v'v''j'j''}(T) = \left[\frac{N_{tot} - N^x_{v'v''j'j''}(T)}{N_{tot} N^x_{v'v''j'j''}(T)}\right]^{1/2} \sigma^x_{v'v''j'j''}(T). \tag{9}$$

Upon evaluation, Eq. (7) assumes the form

$$k^x_{v'v''j'j''}(T) = g_e\left(\frac{8kT}{\pi\mu_{O_2-O_2}}\right)^{1/2} \sigma^x_{v'v''j'j''}(T). \tag{10}$$

To study the overall effect of the rotational excitation on the kinetics of the title reaction, we have calculated also the rotationally-averaged rate constant for specific vibrational combinations, $k^x_{v'v''}(T)$. Once again, the direct QCT method has been used and we have obtained a formula similar to Eq. (10) for $k^x_{v'v''}(T)$,

$$k^x_{v'v''}(T) = g_e\left(\frac{8kT}{\pi\mu_{O_2-O_2}}\right)^{1/2} \sigma^x_{v'v''}(T), \tag{11}$$

where the $\sigma^x_{v'v''}$ are estimated using the direct QCT method: for each trajectory, the initial rotational quantum number and the initial translational energy are randomly generated in accordance with the corresponding thermal distributions for a given temperature. In the remaining of this section, we summarize the procedures used to generate the probability distributions for the initial rotational quantum numbers and translational energy (see also Ref. [23]). Note that to calculate the vibrationally averaged thermal rate coefficient one requires also the initial distribution for the vibrational quantum numbers of $O_2(v')$ and $O_2(v'')$. This will be examined later in Section 3.

The rotational distribution is given by

$$P(j) = \frac{(2j+1)\exp[-j(j+1)B_v/kT]}{\sum_j (2j+1)\exp[-j(j+1)B_v/kT]}, \tag{12}$$

where $2j+1$ is the rotational degeneracy factor, and B_v the rotational constant. For O_2 the summation includes only odd j states. According to this distribution the initial rotational states are selected from

$$j = \tfrac{1}{2}\left\{1 - \frac{4kT}{B_v}\ln[\xi(X_{max} - X_{min}) + X_{min}]\right\}^{1/2} - \tfrac{1}{2}, \tag{13}$$

where the random number ξ has the uniform distribution in the interval $0 \le \xi \le 1$. X_{max} and X_{min} are dimensionless quantities defined by

$$X_{max} = \exp[-j_{max}(j_{max}+1)B_v/kT], \tag{14}$$

$$X_{min} = \exp[-j_{min}(j_{min}+1)B_v/kT], \tag{15}$$

where $j_{min} = 1$, and j_{max} is some maximum value of j; this can be taken as some large value of j or, e.g., the smallest value of j for which $(2j+1)\exp[-j(j+1)B_v/kT] \le 10^{-4}$. As usual, the rotational quantum number j is then obtained by rounding-off the real j so obtained to its nearest integer, and selected only the odd values by using $j = 2\,\mathrm{int}(j/2) + 1$ where $\mathrm{int}(x)$ means the integer part of x.

Similarly, the probability distribution to be simulated for the initial translational energy is

$$P(E_{tr})\,dE_{tr} = \left(\frac{1}{kT}\right)^2 E_{tr}\exp(-E_{tr}/kT)\,dE_{tr}. \tag{16}$$

According to this distribution, the initial translational energy E_{tr} for each trajectory can be selected from

$$1 - \left(1 + \frac{E_{tr}}{kT}\right)\exp(-E_{tr}/kT) - \xi = 0, \tag{17}$$

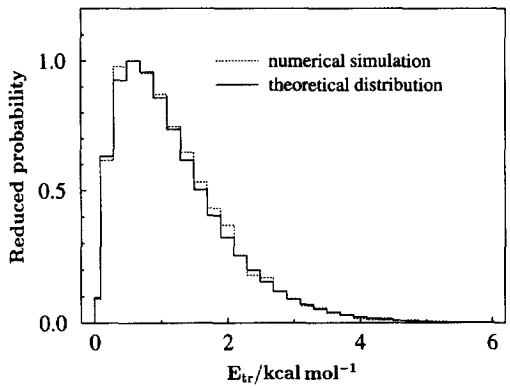

Fig. 1. Initial translational energy distribution. The solid line represents the theoretical distribution of Eq. (16), while the dotted line shows the results based on a computer simulation employing 10,000 trajectories.

an equation which can easily be solved by using the Newton-Raphson method once the random number ξ and the temperature are specified. As shown in Fig. 1, the simulated distribution shows good agreement with the exact one when a batch of 10,000 trajectories is employed for the calculations.

3. Results and discussion

To compare with the results reported in paper I, we have calculated rotational-specific rate constants $\left[k^{x}_{v'v''j'j''}(T)\right]$ and rotationally-averaged rate constant $\left[k^{x}_{v'v''}(T)\right]$ for the vibrational combinations (27,15) and (27,27) at three temperatures: 150, 300 and 500 K. For brevity, we have fixed in the former calculations the rotational quantum number at $j' = j'' = 9$, which is the most populated rotational state at such temperatures. Batches of 200 trajectories each have been employed to determine by trial-and-error the maximum impact parameter, $b_{max}(T)$. The calculated optimum values of $b_{max}(T)$ are listed in Table 1. They are found to decrease with temperature for both vibrational combinations. Since the average initial translational energy E_{tr} increases with temperature, such a trend mimics that found in our previous state-to-state calculations which show b_{max} to decrease with initial translational energy.

Batches of 2,000 trajectories have then been run for each initial vibrational combination. Tables 1 and 2 report summaries of the trajectory calculations while the calculated rate constants are displayed in Figs. 2 and 3. The notable feature from Tables 1 and 2 is the fact that the cross sections for dissociation dominate while the exchange cross sections are typically very small even when compared with those for excited ozone formation.

Table 1
Summary of the trajectory calculations with the quantum rotational state of the colliding O_2 molecules fixed at $j' = j'' = 9$.

T (K)	b_{max} (Å)	$\sigma^{\star}_{v'v''j'j''}$ (Å^2)	$\sigma^{diss}_{v'v''j'j''}$ (Å^2)	$\sigma^{exc}_{v'v''j'j''}$ (Å^2)
$v' = 27$ and $v'' = 15$				
150	6.75	0.286 ± 0.142	1.002 ± 0.267	0
300	4.75	0.248 ± 0.094	1.240 ± 0.208	0.035 ± 0.035
500	3.50	0.192 ± 0.061	1.097 ± 0.143	0.077 ± 0.038
$v' = 27$ and $v'' = 27$				
150	7.00	3.618 ± 0.521	19.319 ± 1.140	0.462 ± 0.188
300	5.75	3.584 ± 0.424	15.840 ± 0.835	0.623 ± 0.179
500	5.25	4.070 ± 0.410	12.339 ± 0.677	0.303 ± 0.114

Fig. 2 shows the calculated rate constants for the vibrational combination (27,15). The results for the rotational combination ($j' = j'' = 9$) rate constants are indicated by the squares, while the rotationally averaged rate constants are shown by the solid dots. Also included for comparison in Fig. 2 are the results previously reported in paper I for $j' = j'' = 1$, which are represented by the solid line. It is seen that increasing the rotational quantum numbers from $j' = j'' = 1$ to $j' = j'' = 9$ leads to some decrease of the rate contants for $O_3^{\star}$ formation and dissociation. It is also seen that the rotationally-averaged rate contants approximately coincide with those reported in paper

Table 2
Summary of the rotationally averaged trajectory calculations.

T (K)	b_{max} (Å)	$\sigma^{\star}_{v'v''}$ (Å^2)	$\sigma^{diss}_{v'v''}$ (Å^2)	$\sigma^{exc}_{v'v''}$ (Å^2)
$v' = 27$ and $v'' = 15$				
150	6.75	0.143 ± 0.101	1.932 ± 0.369	0.072 ± 0.072
300	4.75	0.496 ± 0.132	2.127 ± 0.270	0.106 ± 0.061
500	3.50	0.366 ± 0.084	1.597 ± 0.172	0.019 ± 0.019
$v' = 27$ and $v'' = 27$				
150	7.00	5.080 ± 0.615	22.013 ± 1.205	0.616 ± 0.217
300	5.75	4.934 ± 0.494	18.541 ± 0.889	0.675 ± 0.187
500	5.25	3.897 ± 0.401	15.889 ± 0.750	0.433 ± 0.136

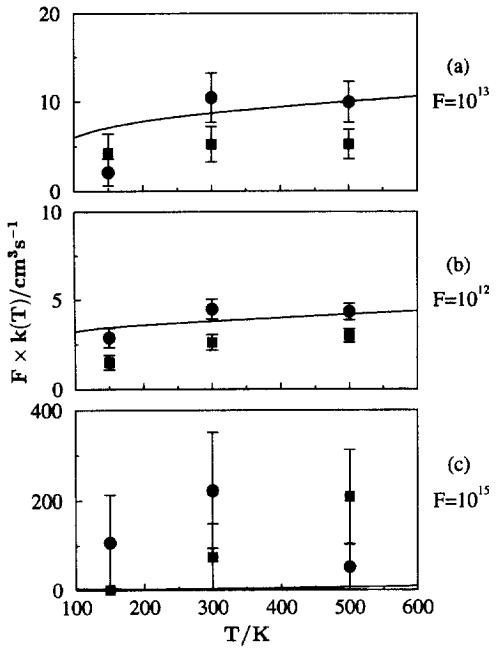

Fig. 2. Calculated vibrationally resolved rate constants $F \times k(T)$ for $v' = 27, v'' = 15$: (a) $O_2(v') + O_2(v'') \rightarrow O_3 + O$ and $O_2(v') + O_2(v'') \rightarrow O_3^* + O$; (b) $O_2(v') + O_2(v'') \rightarrow O_2 + O + O$; (c) $O_2(v') + O_2(v'') \rightarrow O_2 + O_2$. The solid lines refer to the results of paper I which have ignored rotational excitation of the reactant molecules while the symbols stand for the calculations of the present work: the solid squares are for rotational-specific ($j' = j'' = 9$) rate constant and the solid dots for the rotationally-averaged rate constant. The appropriate F factors are indicated in each panel.

I within the statistical error bounds of the calculations. In both cases, the rate constants for the oxygen-atom exchange reaction is predicted to be larger (although affected by considerable error margins) than the value obtained from the ground rotational state calculations [15].

Fig. 3 displays the rate constants for the vibrational combination (27,27). As in Fig. 2, the rotational-specific ($j' = j'' = 9$) rate constans are represented by the solid squares while the rotationally-averaged rate constants are indicated by the solid dots. The rotationally-averaged rate constant for excited ozone formation is now found to be smaller than that reported in paper I by neglecting initial rotational excitation of the O_2 molecules. A similar trend is observed for the dissociation rate constant although the inclusion of rotational excitation leads to rate constants about 30–40% smaller than before [15] over the range of temperatures studied in the present work. It is also seen that the rotational-specific rate constants are now even lower than the rotationally-averaged rate constants for all three types of reactions. Similarly to what has been described for the vibrational combination (27,15), both rotationally averaged and rotational-specific rate constants for the oxygen-atom exchange reaction are found to be larger than those reported in paper I.

In summary, for the rate constants of the above two specific vibrational combinations, the rotational-specific rate constants ($j' = j'' = 9$) are found to be lower than the rate constants assuming ground rotational oxygen molecules. However, the overall effect due to inclusion of rotational excitation into the O_2 colliding partners is seem to be small, since the rotationally-averaged rate constants differ only slightly from the results reported in paper I. In fact, the relative magnitudes of the calculated rate constants remain essentially unaltered by rotationally averaging. Thus, we conclude that initial rotational excitation of the reactant molecules introduces no drastic effects on the rate constants of the title

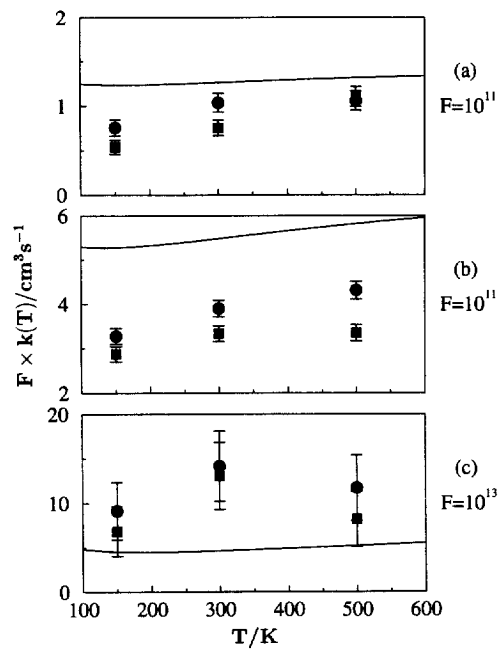

Fig. 3. Calculated vibrationally resolved rate constants for $v' = 27, v'' = 27$. The panels for the different reactions and the symbols are as in Fig. 2.

reaction, at least for the high vibrational combinations (27,15) and (27,27) considered in the present work. It should also be emphasized that no stable ozone molecules (i.e., 'dir' type products) have been produced for both vibrational combinations studied in the present work, a result which is also in agreement with the findings of paper I.

We have also calculated the vibrationally averaged rate constants by the direct QCT approach using a rejection method [24] to sample the vibrational combinations of the two colliding O_2 molecules for each trajectory. However, since we follow paper I and assume a non-LTE condition [16] for the title reaction, the vibrational simulation has been chosen to mimic the experimental bimodal distribution obtained by Miller et al. [2] (see Fig. 4) in the photolysis of ozone at 226 nm. A total of 10,000 trajectories has been run for each temperature, being the results reported in Table 3 and Fig. 5. As shown, the calculated vibrationally averaged rate constants for dissociation and $O_3^\star$ formation are of the same order of magnitude as those reported in paper I, although differences are clearly visible. Most significant is the fact that the vibrationally averaged rate coefficients for $O_3^\star$ formation show a markedly different temperature dependence, with the rate constant decreasing with temperature. Such a difference may be attributed to rotational effects for low vibrational combinations of the colliding O_2 molecules, which have not been directly studied in the present work. Indeed, we have previously found for vibrational combinations lower than (27,15) [e.g., (27,10) in Table 1 of paper I] that a threshold translational energy of at least 1 kcal mol^{-1} is required for reaction to take place. It is therefore plausible to expect that rotational excitation of the reactant oxygen molecules may play a role for such vibrational combinations. On the one hand, the assumption that conversion of rotational in translational energy can be effective would be expected to increase the rate of reaction. On the other hand, for a reaction with a

Table 3
Summary of the vibrational-rotationally averaged trajectory calculations.

T (K)	b_{max} (Å)	$\sigma^\star$ (Å^2)	σ^{diss} (Å^2)	σ^{exc} (Å^2)
150	7.00	0.493 ± 0.087	1.462 ± 0.149	0
300	5.75	0.291 ± 0.055	0.997 ± 0.101	0
500	5.25	0.121 ± 0.032	0.753 ± 0.080	0.035 ± 0.017

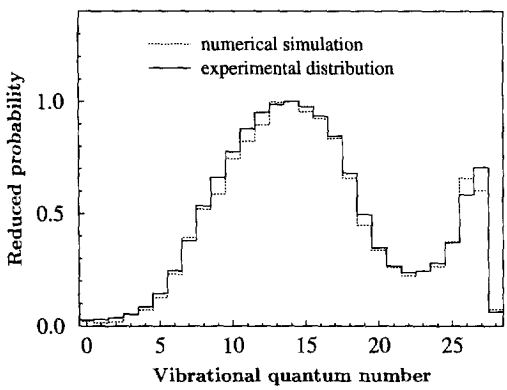

Fig. 4. Initial vibrational distribution of the reactant O_2 molecules. The solid line represents the experimental distribution obtained in the photolysis of O_3 [2] at 226 nm, while the dotted line shows the results of the computer simulation of the present work based on 10,000 trajectories.

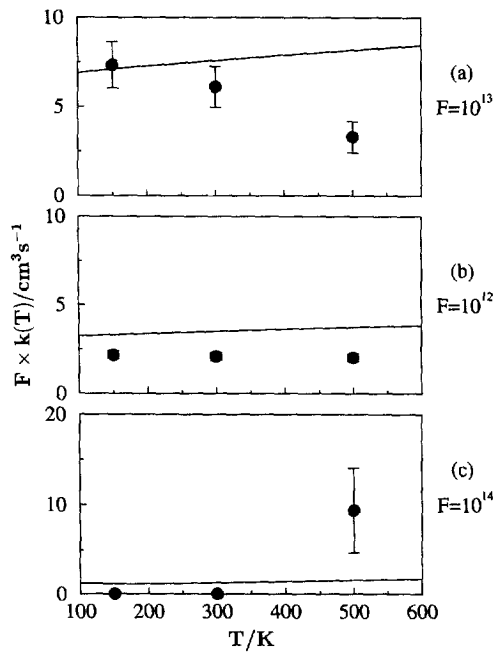

Fig. 5. Vibrationally averaged rate constants based on the experimental bimodal distribution of Miller et al. [2]. The panels for the different reactions are as in Fig. 2. The solid dots are for the present results. Note that in pannel (b) the error margins are contained within the size of the dots.

narrow cone of acceptance such as the title one, the inclusion of rotational excitation tends to dealign the reactant molecules from the most favorable orientation for reaction and hence inhibit direct $O_3^\star$ formation. This seems to dominate for low initial vibrational states whose probability is known to peak in the vicinity of $v = 14$ (see Fig. 4). Moreover, our previous rotationless calculations [15] are seen to overestimate the results from the present work for the dissociation rate constant by $20 - 40\%$. This suggests that the effect of rotational excitation on the overall production of odd oxygen should be of the same order of magnitude over the range of temperatures considered in the present work. Thus, a probably realistic statement is that rotational excitation tends to inhibit the title reaction by at least 20%, a factor which is predicted to increase with temperature.

4. Conclusions

As in paper I, the vibrationally resolved rate constants calculated for the title reaction have been shown to vary drastically with the vibrational combination of the reactant O_2 molecules. Similarly, among the three possible reactive channels, dissociation to $O_2 + O + O$ has been found to dominate while the exchange reaction was essentially negligible. Regarding the rotational excitation of the colliding O_2 molecules, it has been shown to have no effect on the order of magnitude of the calculated rate constants for dissociation, and excited ozone $O_3^\star$ formation. This by no means implies that rotational excitation of the colliding O_2 molecules plays no significant role on the kinetics of the title reactions. Indeed, Fig. 5 suggests that it may be responsible for the marked differences on the temperature dependence of the vibrationally averaged rate constant for $O_3^\star$ formation. Moreover, it has been shown to inhibit the dissociation reaction by a factor of $20 - 40\%$ over the range of temperatures considered in the present work.

A final comment goes to the possible implications of the title reactions on stratospheric ozone concentration. Clearly, since our main conclusions agree well with those reported in paper I, we reiterate that they should be taken in consideration in modelling the ozone budget. In fact, even if inelastic processes may explain the observed jump in $O_2(v \geq 26)$ depletion [12] in collisions with O_2, the present calculations suggest that odd-oxygen (and hence ozone) can be formed from reactions involving highly vibrationally excited oxygen molecules.

Acknowledgements

We thank the authors of Ref. [12] for bringing their work to our attention prior to publication. This work has been supported by the Fundação para a Ciência e Tecnologia, Portugal, under programmes PRAXIS XXI and FEDER (Contract 2/2.1/QUI/408/94).

References

[1] T.G. Slanger, Science 265 (1994) 1817.
[2] R.L. Miller, A.G. Suits, P.L. Houston, R. Toumi, J.A. Mack, A.M. Wodtke, Science 265 (1994) 1831.
[3] P. Crutzen, Science 277 (1997) 1951.
[4] J.M. Price, J.A. Mack, C.A. Rogaski, A.M. Wodtke, Chem. Phys. 175 (1993) 83.
[5] C.A. Rogaski, J.M. Price, J.A. Mack, A.M. Wodtke, Geophys. Res. Lett. 20 (1993) 2885.
[6] H. Parker, T.G. Slanger, J. Chem. Phys. 100 (1994) 287.
[7] M. Klatt, I.W.M. Smith, R.P. Tuckett, G.N. Ward, Chem. Phys. Lett. 224 (1994) 253.
[8] C.A. Rogaski, J.A. Mack, A.M. Wodtke, Faraday Discuss. Atmos. Chem. 100 (1995) 229.
[9] N. Balakrishnan, G.D. Billing, Chem. Phys. Lett. 242 (1995) 68.
[10] A.J.C. Varandas, A.A.C.C. Pais, in: S.J. Formosinho, I.G. Czismadia, L.G. Arnaut (Eds.), Theoretical and Computational Models for Organic Chemistry, Kluwer, Dordrecht, 1991, p. 55.
[11] N. Balakrishnan, G.D. Billing, J. Chem. Phys. 189 (1994) 2785.
[12] J. Campos-Martínez, E. Carmona-Novillo, J. Echave, M.I. Hernández, R. Hernández-Lamoneda, J. Palma, Mol. Phys., submitted for publication.
[13] D.M. Lauvergnat, D.C. Clary, J. Chem. Phys. 108 (1998) 3566.
[14] J.A. Mack, Y. Huang, A.M. Wodtke, G.C. Schatz, J. Chem. Phys. 105 (1997) 7495.
[15] A.J.C. Varandas, W. Wang, Chem. Phys. 215 (1997) 167.
[16] X. Yang, J.M. Price, J.A. Mack, C.G. Morgan, C.A. Rogaski, D. McGuire, E.H. Kim, A.M. Wodtke, J. Phys. Chem. 93 (1993) 3944.

[17] W. Wang, R. González-Jonte, A.J.C. Varandas, J. Phys. Chem., in press.
[18] W.L. Hase, MERCURY: a general Monte-Carlo classical trajectory computer program, QCPE#453. An updated version of this program is VENUS96: W.L. Hase, R.J. Duchovic, X. Hu, A. Komornik, K.F. Lim, D.-H. Lu, G.H. Peslherbe, K.N. Swamy, S.R. van de Linde, A.J.C. Varandas, H. Wang, R.J. Wolf, QCPE Bull 16 (1996) 43.
[19] A.J.C. Varandas, Adv. Chem. Phys. 74 (1988) 255.
[20] A.J.C. Varandas, in: G. Delgado-Barrio (Ed.), Dynamical Processes in Molecular Physics, IOP Publishing, Bristol, 1993, p. 3.
[21] H. Szichman, A.J.C. Varandas, M. Baer, Chem. Phys. Lett. 231 (1994) 253.
[22] H. Szichman, A.J.C. Varandas, M. Baer, J. Chem. Phys. 102 (1995) 3474.
[23] A.J.C. Varandas, J. Brandão, M.R. Pastrana, J. Chem. Phys. 96 (1992) 5137.
[24] D.L. Bunker, Meth. Comp. Physics 10 (1971) 287.